

**GEOLOGIC MAPPING (1:60K) OF AEOLIS MONS, GALE CRATER, MARS AND SPECTRAL INTERPRETATION OF MAP UNITS.** D. L. Buczowski<sup>1</sup>, I. E. Ettenborough<sup>2</sup>, K. D. Seelos<sup>1</sup>, B. J. Thomson<sup>2</sup> and L. S. Crumpler<sup>3</sup>, <sup>1</sup>JHU Applied Physical Laboratory, 11100 Johns Hopkins Rd., Laurel, MD 21043 (debra.buczowski@jhuapl.edu); <sup>2</sup>University of Tennessee, Knoxville, TN; <sup>3</sup>New Mexico Museum of Natural History & Science, Albuquerque, NM.

**Introduction:** Aeolis Mons (Fig. 1a) is a ~5 km-high stack of layered materials superposed on the floor and central peak of Gale crater (5.3°S, 137.8°E). Since landing in 2012, the Mars Science Laboratory (MSL) Curiosity rover is investigating the crater floor and the lower units of Aeolis Mons in the northwestern portion of Gale crater [e.g., 1]. However, studies of the remainder of Gale consists largely orbital identification of minerals such as hematite, mono- and polyhydrated sulfates, Fe/Mg-phyllsilicates, and hydrated silica [e.g., 2–7]. These minerals indicate significant past aqueous activity under variable geochemical conditions.

We are constructing a geologic map of the western portion of the Gale mound at 1:60K scale. The overarching goal of the project is to better understand the origin(s) of mound-forming and mound-draping layers. Coupled with the geomorphic mapping efforts, we correlate mapped units to Compact Reconnaissance Imaging Spectrometer for Mars (CRISM) [4] near-infrared spectral data in order to assess the primary and secondary mineral budgets.

The lower units of Gale are the subject of considerable interest because they capture a transition from an environment that appears to have favored phyllosilicate-bearing layers to an environment that favored the deposition of sulfate-bearing layers [2,5,6]. More detailed mapping of this transition zone will reveal if the transition was one-sided and irreversible [e.g., 8,9], or if simultaneous or near-contemporaneous deposition of phyllosilicates and sulfate occurred [10].

We here present the results of geologic mapping in the southwestern region of Aeolis Mons, where geomorphic units are closely related to mineralogic detections, and can be mapped for significant distances around the mound.

**Methods:** The geomorphic map has been created using traditional geomorphic mapping principles, but also informed by the addition of CRISM compositional data. The basemap was a 5 m/pixel Context Camera (CTX) mosaic; a ~25 cm/pixel HiRISE merged orthophoto mosaic [11] was also used for the northern part of the map region (Fig. 1). HRSC and HiRISE stereo-derived topography (post spacing 1 m and 50 m, respectively) were also utilized. Units contacts have been drawn throughout the map region. Different team members mapped in three different regions (Fig. 1); these contacts are being reconciled now. Unit descriptions are also ongoing.

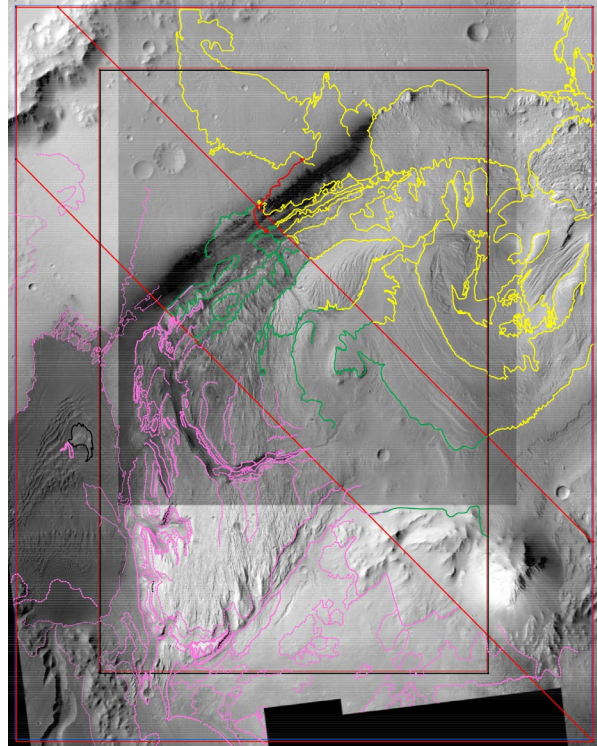


**Figure 1.** CTX mosaic of western Aeolis Mons overlain by darker HiRISE mosaic (upper center). Inner black box marks map region. Red diagonal lines mark the map areas of 3 team members, with contacts in yellow, green or pink. Some overlap was purposely mapped.

To characterize the spatial distribution of Fe/Mg-phyllsilicates, mono- and polyhydrated sulfates, and hematite in Gale crater we utilized hyperspectral visible-near infrared (0.4–4.0  $\mu\text{m}$ ) data acquired by CRISM. Data included 18 or 36 m/pix resolution targeted images processed through the Map-Projected Targeted Reduced Data Record (MTRDR) pipeline [12]; CRISM data were photometrically and atmospherically corrected, noise filtered, and map projected. Summary parameters images [13] were also generated.

We then created two qualitatively balanced CRISM mosaics of red-green-blue (RGB) summary parameter browse images [14]. Because each image is georeferenced to align with the CTX basemap, we are able to use these mosaics to facilitate improved correlation to surface morphology. The first RGB mosaic is composed of the summary parameters D2300, SINDEXT, and BD1900, respectively [13]; in this color composite,

Fe/Mg phyllosilicates appear red or purple while sulfates appear yellow-green. The second mosaic is composed of the summary parameters SINDEXT, BD2100 and BD1900 [13]; in this color composite, monohydrated sulfates are yellow, while polyhydrated sulfates appear magenta.

**Sedimentary layering in Aeolis Mons:** The kilometers-thick sedimentary sequence in Aeolis Mons has been previously recognized to record a transition from a climate favorable to the formation of clays to a climate more favorable to the formation of sulfates [2]. However, more recent studies suggest that the “layer-cake” style stratigraphic sequences interpreted from orbital maps are not entirely consistent with Curiosity rover observations of the Bradbury Rise in NW Gale crater [14, 15].

*In Map Region:* An extended distribution of hematite-bearing outcrops has been identified around Aeolis Mons [14]. In the northwest of the map region, close to Curiosity’s traverse, the hematite-bearing Vera Rubin Ridge stands in high relief compared to its surroundings. To the northwest of the ridge, hematite is located in a nearly flat-lying deposit with dunes and other units superposed. Moving south, a hematite signature becomes associated with an erosional trough and narrowly outcropping along the side of Aeolis Mons. A second, higher elevation hematite-bearing layer becomes apparent further south.

The southwestern lobe of Aeolis Mons shows additional stratigraphic layering along its margins [17]. A relatively high-albedo unit is observed at the toe of the lobe; two medium-albedo units are observed above the bright unit, while a third medium-albedo unit is observed below it. All units show internal layering and possible cross-bedding. The high-albedo unit appears to be stripped back, as if the toe has been heavily eroded.

While there is no CRISM coverage at the toe, the high-albedo unit can be followed north along the exterior of the SW Aeolis margin. As revealed in the summary parameter images, the high albedo unit corresponds to a Fe/Mg-phyllsilicate bearing layer. Above this is a monohydrated sulfate-bearing layer, while a layer of polyhydrated sulfates is at the top of the stack.

These same layers can followed further can be seen inside the canyons cutting Aeolis Mons within the map region. Creating a geologic cross section across the larger canyon shows that the layers, defined by both geomorphology and mineralogy, in this region of Aeolis Mons do seem to have a tilted “layer-cake” style orientation [17]. The layers exposed in the smaller, southern canyon are consistent with those in the larger, northern canyon if it is assumed that the layers have moved downwards along a fault or slump scarp.

If this interpretation of the geomorphology, mineralogy, and topography of SW Aeolis Mons is accurate, then this region is very different from NW Aeolis [14]. However, more work is needed before we can determine what the difference between this cross-section and the Bradbury Rise cross-section [15] means towards the formation of Aeolis Mons.

*Outside of map region:* The two hematite layers observed in the map region are particularly distinct on the far southeastern lobe of Aeolis Mons [14]; the upper of these two layers is expressed as a more erosionally resistant ridge. These observations indicate that the process(es) responsible for hematite formation were active throughout the lower mound. Understanding additional stratigraphic and mineralogic associations will further inform potential formation scenarios.

As with the southwestern lobe in the map region, layers of monohydrated and polyhydrated sulfates over another hydrated material (possibly Fe/Mg-phyllsilicate) have also been detected on the southeastern lobe of Aeolis Mons [18]. However, unlike in the map region, in the southeastern lobe the monohydrated sulfates appear to be stratigraphically above the polyhydrated sulfates. We have yet to determine what this change in layering means toward understanding the stratigraphic history of Aeolis Mons.

**Acknowledgments:** This work was funded by grant #80NSSC17K0647 through the NASA Mars Data Analysis Program, and through the MRO CRISM investigation, JPL sub-contract 1277793 to JHU/APL.

**References:** [1] Grotzinger J.P. et al. (2015) *Science* 350, aac7575. [2] Milliken R.E. et al. (2010) *GRL* 37, L04201. [3] Ehlmann B.L. & Buz J. (2015) *GRL* 42, 264–273. [4] Murchie S.L. et al. (2007) *JGR* 112, E05S03. [5] Anderson R.C., and J.F. Bell III (2010), *Mars* 5, 76–128. doi: 10.1555/mars.2010.0004 [6] Thomson B.J. et al. (2011) *Icarus* 214, 413–432. [7] Sheppard R. Y. et al. (2021) *JGR: Planets*, 126(2). doi: 10.1029/2020JE006372 [8] Bibring, J.-P. et al. (2006) *Science* 312(5772), 400–404. [9] Murchie S. L. et al. (2009) *JGR* 114, E00D06. doi: 10.1029/2009JE003342 [10] Baldrige A. M. et al. (2009) *GRL* 36, 19201. doi:10.1029/2009GL040069 [11] Calef III F. J. & Parker T. (2016) MSL Gale Merged Orthophoto Mosaic. PDS Annex, USGS [12] Seelos F.P. et al. (2012) *Plan. Data Users Wksp.* [13] Viviano-Beck C.E. et al. (2014) *JGR* 119, 1403–1431. [14] Seelos K.D. et al. (2019) *LPSC*, abs. 2785. [15] Stack K.M. et al. (2016) *Icarus*, 280, 3–21. [16] Rapin, W.G. et al. (2021) *Geology* 49. doi: 10.1130/G48519.1 [17] Buczkowski D.L. et al. (2020) *LPSC*, abs. 2664. [18] Ettenborough I.E. et al. (2021) *LPSC*, abs. 2308.